

LOS-based Conjugate Beamforming and Power-Scaling Law in Massive-MIMO Systems

Dian-Wu Yue, *Member, IEEE*, and Geoffrey Ye Li, *Fellow, IEEE*

Abstract

This paper is concerned with massive multiple-input multiple-output (MIMO) systems over Rician flat fading channels. In order to reduce the overhead to obtain full channel state information and to avoid the pilot contamination problem, by treating the scattered component as interference, we investigate a transmit and receive conjugate beamforming (BF) transmission scheme only based on the line-of-sight (LOS) component. Under Rank-1 model, we first consider a single-user system with N transmit and M receive antennas, and focus on the problem of power-scaling law when the transmit power is scaled down proportionally to $\frac{1}{MN}$. It can be shown that as MN grows large, the scattered interference vanishes, and the ergodic achievable rate is higher than that of the corresponding BF scheme based fast fading and minimum mean-square error (MMSE) channel estimation. Then we further consider uplink and downlink single-cell scenarios where the base station (BS) has M antennas and each of K users has N antennas. When the transmit power for each user is scaled down proportionally to $\frac{1}{MN}$, it can be shown for finite users that as M grows without bound, each user obtains finally the same rate performance as in the single-user case. Even when N grows without bound, however, there still remains inter-user LOS interference that can not be cancelled. Regarding infinite users, there exists such a power scaling law that when K and M^α go to infinity with a fixed and finite ratio for a given $\alpha \in (0, 1)$, not only inter-user LOS interference but also fast fading effect can be cancelled, while fast fading effect can not be cancelled if $\alpha = 1$. Extension to multi-cells and frequency-selective channels are also discussed shortly. Moreover, numerical results indicate that spacial antenna correlation does not have serious influence on

Dian-Wu Yue is with the College of Information Science and Technology, Dalian Maritime University, Dalian, Liaoning 116026, China (e-mail: dwyue@dlmu.edu.cn). Geoffrey Ye Li is with School of Electrical and Computer Engineering, Georgia Institute of Technology, Atlanta, GA 30332-0250, USA (Email:liye@ece.gatech.edu)

the rate performance, and the BS antennas may be allowed to be placed compactly when M is very large.

Index Terms

Massive-MIMO, Rician fading, beamforming, power scaling, line-of-sight, spacial correlation

I. INTRODUCTION

Wireless transmission using multiple antennas has attracted much interest in the past couple of decades due to its capability to exploit the tremendous capacity inherent in MIMO techniques. Various aspects of wireless MIMO systems have been studied intensively, especially the important capacity aspect [1]. Whilst single-user systems have been well investigated, multi-user systems including classical uplink (multiple access) and downlink (broadcast) systems nowadays have become the focus of theoretical analysis and practical design of MIMO communications [2]. Theoretically, the maximum-likelihood multiuser detector and “dirty paper coding” can be used to obtain optimal performance for the uplink and downlink systems, respectively. However, they induce a significant complexity burden on the system implementation, especially for a large multiple antenna system. Therefore, linear effective processing schemes, in particular beamforming (BF) and zero-forcing (ZF) detecting or precoding, are of particular interest as low-complexity alternatives [3] - [8].

Recently, there exist a lot of interests in multiuser MIMO with a very large antenna array at the base station (BS), which means a array comprising a few hundreds of antennas simultaneously serving tens of users [9] - [25]. These large scale MIMO systems can offer much higher data rates, increased link reliability, and potential power savings since the transmitted RF energy can be more sharply focused in space while many random impairments can be averaged out, which is a critical difference from the traditional MIMO systems. It should be pointed out that these benefits of large-scale antenna arrays can be reaped by using the simple BF or ZF processing [9], [24].

The analysis and design of massive MIMO systems is at the moment a fairly new research topic [10]. In [12], linear precoding performance is studied for measured very-large MIMO downlink channels. It is shown that there exist clearly benefits with an excessive number of BS antennas [12]. In [13], [14] and [15], with simple linear BF and ZF receivers authors give uplink

capacity analysis of single-cell, single-cell distributed, and multi-cell very large MIMO systems, respectively, derive bounds on the achievable sum rate in both small and large-scale fading environments, and provide asymptotic performance results when the number of antennas grows without bound. In [16], authors provide a unified analysis of the uplink and downlink performance of linear processing in multi-cell systems when the number of the BS antennas and the number of users both grow large with a fixed ratio, and derive asymptotically tight approximations of the achievable rates under a realistic system model which accounts for channel estimation, pilot contamination, path loss, and antenna correlation.

In order to achieve the performance predicted by the mentioned-above analysis results, BS must acquire channel state information (CSI). In practice, however, the BS does not have perfect CSI [19]. Instead, it estimates the channels. The conventional way of doing this is to use uplink pilots. If channel coherence time is limited, the number of possible orthogonal pilot sequences is limited too and hence, pilot sequences have to be reused in other cells. Therefore, channel estimates obtained in a given cell will be contaminated by pilots transmitted by users in other cells [19]. This causes pilot contamination. The effect of pilot contamination appears to be a fundamental challenge of massive-MIMO system design, which warrants future research on the topic [9], [10], [17], [18].

So far there have appeared most of research results on the massive MIMO based on the ground of Rayleigh fading (see [9] - [18] and references therein among others). However, despite their practical significance, and in contrast to the Rayleigh fading case, there are currently very few which apply for Rician fading, [20], [21], [22]. In particular, authors in [20] propose a deterministic equivalent of ergodic sum rate and an algorithm for evaluating the capacity-achieving input covariance matrices for uplink massive MIMO systems. In [21], authors study the achievable uplink rates of massive MIMO systems using BF and ZF receivers. Assuming imperfect CSI, they find such a power scaling law that with a non-zero Rician factor, the uplink rates converge to the same constant values when the number of BS antennas M grows large if the needed transmit power of each user is scaled down proportionally to $1/M$. However, in pure Rayleigh fading environment, the corresponding transmit power can only be scaled down by a factor of $1/\sqrt{M}$ [13], [21].

The Rician fading model is also very important and applicable when the wireless link between the transmitter and the receiver has a direct path component in addition to the diffused Rayleigh

component. It can be employed in diverse modern applications, like suburban/indoor WLANs or 60 GHz communications, to deliver ultra-broadband data rates [26]. Another emerging applications are typical point-to-point microwave links and MIMO vehicular networks, where a moving vehicle communicates with either another vehicle or with the roadside in support of demanding applications spanning high-speed networking and video streaming to mobile commerce and Web surfing [26]. Moreover, it is also suitable for application in small cell networks [27]. With decreasing cell sizes, the user terminal are likely to have line-of-sight (LOS) links to one or several BSs. This means the the normally fast-fading wireless channel contains strong deterministic non-fading components [27], [28].

For this reason, we are concerned with massive-MIMO systems over Rician fading channels in this paper. In order to avoid the pilot contamination problem, we treat the scattered component as interference, and study a transmit and receive BF transmission scheme only based on the LOS component. In what follows, we first consider a single-user MIMO system, and then consider uplink and downlink scenarios in a single-cell MIMO network.

II. SINGLE-USER MASSIVE-MIMO SYSTEMS

A. Single-User System Model

We consider a single-user MIMO system with N transmit antennas and M receive antennas. Then $M \times 1$ received signal vector is represented as

$$\mathbf{y} = \sqrt{p_u} \mathbf{G} \mathbf{x} + \mathbf{z} \quad (1)$$

where p_u is the average transmitted power of the single user; \mathbf{G} is the $M \times N$ channel matrix such that $[\mathbf{G}]_{mn} = g_{mn}$, and g_{mn} represents the channel coefficient between the m -th receive antenna and n -th transmit antenna; \mathbf{x} is the symbol vector transmitted by the user; and \mathbf{z} is a vector of zero-mean additive white Gaussian noise (AWGN) with covariance matrix $\mathbb{E}[\mathbf{z}\mathbf{z}^H] = \mathbf{I}_M$.

Taking into account the effects of fast fading, geometric attenuation, and shadow fading, the entry g_{mn} of \mathbf{G} should be modelled as

$$g_{mn} = h_{mn} \sqrt{\beta} \quad (2)$$

where h_{mn} represents the fast fading coefficient from the n -th transmit antenna to the m -th receive antenna, and β models the geometric attenuation and shadow fading, which is independent over

m and n . Therefore, we have

$$\mathbf{G} = \sqrt{\beta} \mathbf{H} \quad (3)$$

where $\mathbf{H} = [h_{mn}]$.

We assume that the fast fading is Rician frequency-flat. Then the matrix \mathbf{H} can be decomposed into a sum of a specular matrix and a scattered matrix, i.e.,

$$\mathbf{H} = \sqrt{\bar{\vartheta}} \bar{\mathbf{H}} + \sqrt{\tilde{\vartheta}} \tilde{\mathbf{H}} \quad (4)$$

where $\bar{\vartheta} = \frac{\vartheta}{1+\vartheta}$, $\tilde{\vartheta} = \frac{1}{1+\vartheta}$, and $\vartheta \geq 0$ is just the Rician K -factor. Note that $\vartheta = 0$ corresponds to a Rayleigh fading while $\vartheta \rightarrow \infty$ corresponds to non-fading channels. In this paper, we always assume that $\vartheta > 0$. The specular matrix $\bar{\mathbf{H}}$ in (4) is given by [29] - [31]

$$\bar{\mathbf{H}} = \mathbf{r} \mathbf{t}^T \quad (5)$$

where \mathbf{r} and \mathbf{t} are the specular array responses at receiver and transmitter, respectively, and can be written as

$$\mathbf{r} = [1, e^{j2\pi d_r \sin(\theta)}, \dots, e^{j2\pi(M-1)d_r \sin(\theta)}]^T \quad (6)$$

and

$$\mathbf{t} = [1, e^{j2\pi d_t \sin(\phi)}, \dots, e^{j2\pi(N-1)d_t \sin(\phi)}]^T \quad (7)$$

where θ or ϕ is the angle of arrival or departure of the specular component, and d_r or d_t is the antenna spacing in wavelengths at receiver or transmitter. For the scattered matrix $\tilde{\mathbf{H}}$ in (4), its entries are independent and identically distributed (i.i.d) circular complex Gaussian random variables with zero mean unit variance, i.e., $\tilde{h}_{mn} \sim \text{CN}(0, 1)$.

Through the paper, we assume that neither the transmitter nor the receiver knows the scattered component, but both of them knows the specular component.

B. Transmit/Receive BF Scheme based on the Specular Component

A MIMO system can be configured differently. One configuration is transmit/receive BF which has been widely used due to its simplicity and good performance. It is well known that traditional transmit/receive BF schemes are usually based on the scattered component. In this paper, we investigate a transmit/receive BF scheme only based on the specular component due to the assumption which neither the transmitter nor the receiver knows the scattered component.

Transmit/receive BF system transmits one symbol at a time. We denote by s the desired information symbol such that $\mathbb{E}s^H s = 1$. Then s is first weighted by the transmit beamformer \mathbf{b} with $\mathbb{E}\mathbf{b}^H \mathbf{b} = 1$ before being feeded to the N transmit antennas. Now let

$$\mathbf{g} = \mathbf{G}\mathbf{b} = \sqrt{\bar{\vartheta}\beta}\bar{\mathbf{h}} + \sqrt{\tilde{\vartheta}\beta}\tilde{\mathbf{h}} = \bar{\mathbf{g}} + \tilde{\mathbf{g}} \quad (8)$$

where $\bar{\mathbf{h}} = \bar{\mathbf{H}}\mathbf{b}$ and $\tilde{\mathbf{h}} = \tilde{\mathbf{H}}\mathbf{b}$. Then the received vector in (1) can be rewritten as

$$\begin{aligned} \mathbf{y} &= \sqrt{p_u}\mathbf{g}s + \mathbf{z} \\ &= \sqrt{p_u\bar{\vartheta}\beta}\bar{\mathbf{h}}s + \sqrt{p_u\tilde{\vartheta}\beta}\tilde{\mathbf{h}}s + \mathbf{z} \\ &= \sqrt{p_u\bar{\vartheta}\beta}\bar{\mathbf{h}}s + \bar{\mathbf{z}} \end{aligned} \quad (9)$$

where $\bar{\mathbf{z}} = \sqrt{p_u\tilde{\vartheta}\beta}\tilde{\mathbf{h}}s + \mathbf{z}$. (9) implies that the considered MIMO system can be viewed as a MIMO system operating in a pure LOS environment with additive noise $\bar{\mathbf{z}}$.

After receiving \mathbf{y} , the receiver employs a weighting vector \mathbf{w} to combine \mathbf{y} to a single decision variable. The transmit and receive weighting vectors, \mathbf{b} and \mathbf{w} , should be chosen to maximize the output signal-to-interference-noise ratio (SINR), as defined by [32]

$$\gamma = p_u\beta\bar{\vartheta} \cdot \frac{\mathbf{w}^H(\bar{\mathbf{H}}\mathbf{b})(\bar{\mathbf{H}}\mathbf{b})^H\mathbf{w}}{\mathbf{w}^H\Omega\mathbf{w}} \quad (10)$$

where

$$\begin{aligned} \Omega &= \mathbb{E}\bar{\mathbf{z}}\bar{\mathbf{z}}^H \\ &= \mathbb{E}(\sqrt{p_u\beta\tilde{\vartheta}}\tilde{\mathbf{h}}s + \mathbf{z})(\sqrt{p_u\beta\tilde{\vartheta}}\tilde{\mathbf{h}}s + \mathbf{z})^H \\ &= p_u\beta\tilde{\vartheta}\tilde{\mathbf{h}}\tilde{\mathbf{h}}^H + \mathbf{I}_M. \end{aligned} \quad (11)$$

It should be noticed that neither the transmitter nor the receiver can know Ω , but both of them can know its statistical average $\bar{\Omega}$. Since the $M \times 1$ random vector $\tilde{\mathbf{h}}$ follows a complex Gaussian distribution of mean zero and covariance matrix $\mathbb{E}[\tilde{\mathbf{h}}\tilde{\mathbf{h}}^H] = \mathbf{I}_M$, thus

$$\bar{\Omega} = (p_u\beta\tilde{\vartheta} + 1)\mathbf{I}_M. \quad (12)$$

In (10), we replace Ω by $\bar{\Omega}$ and denote the new expression by $\bar{\gamma}$. Then

$$\bar{\gamma} = \frac{p_u\beta\bar{\vartheta}}{p_u\beta\tilde{\vartheta} + 1} \cdot \frac{\mathbf{w}^H(\bar{\mathbf{H}}\mathbf{b})(\bar{\mathbf{H}}\mathbf{b})^H\mathbf{w}}{\mathbf{w}^H\mathbf{w}}. \quad (13)$$

$\bar{\gamma}$ is an important parameter in the whole paper. We refer to it as the output statistical SINR, and will carry on our analysis with its help.

Based on $\bar{\gamma}$ rather than γ , the optimum weighting vectors \mathbf{b} and \mathbf{w} can be chose as [33]

$$\mathbf{b} = \frac{\mathbf{t}}{\sqrt{N}}, \quad \mathbf{w} = \frac{\mathbf{r}}{\sqrt{M}}. \quad (14)$$

So we have the following result.

Proposition 1: The statistical SINR is given by

$$\bar{\gamma} = \frac{NMp_u\beta\bar{\vartheta}}{1 + p_u\beta\bar{\vartheta}} \quad (15)$$

Through analysis in asymptotic cases, Proposition 1 has the following three corollaries.

Corollary 1: If MN and ϑ are fixed, and $p_u \rightarrow \infty$, then

$$\bar{\gamma} \rightarrow MN\vartheta \quad (16)$$

Corollary 2: If MN , β and p_u are fixed, and $\vartheta \rightarrow \infty$, then

$$\bar{\gamma} \rightarrow MN\beta p_u \quad (17)$$

Corollary 3: If ϑ and β are fixed, and let $E_u = MNp_u$ be fixed and $MN \rightarrow \infty$, then

$$\bar{\gamma} \rightarrow E_u\beta\bar{\vartheta}. \quad (18)$$

We denote the ergodic achievable rate by $R = \mathbb{E} \log_2(1 + \gamma)$. Then we have the following lemma about R .

Theorem 1:

$$\log_2(1 + \bar{\gamma}) \leq R \leq \log_2(1 + \bar{\gamma}^\perp) \quad (19)$$

where $\bar{\gamma}^\perp = E_u\beta\bar{\vartheta}$. Furthermore, if $E_u = MNp_u$ is fixed when $MN \rightarrow \infty$, then

$$\lim_{MN \rightarrow \infty} R = \lim_{MN \rightarrow \infty} \bar{R} = \bar{R}^\perp \quad (20)$$

where $\bar{R} = \log_2(1 + \bar{\gamma})$ and $\bar{R}^\perp = \log_2(1 + \bar{\gamma}^\perp)$.

Proof: By using Jensen's inequality, we obtain the following lower bound on the ergodic achievable rate

$$\begin{aligned} R &\geq \log_2\left(1 + \frac{1}{\mathbb{E}(1/\gamma)}\right) \\ &= \log_2\left(1 + \frac{p_u\beta\bar{\vartheta}MN}{p_u\bar{\vartheta}\mathbb{E}|\mathbf{w}^H\tilde{\mathbf{h}}|^2 + \mathbb{E}|\mathbf{w}^H\mathbf{z}|^2}\right). \end{aligned} \quad (21)$$

Since $\mathbb{E}|\mathbf{w}^H \mathbf{z}|^2 = 1$ and $\mathbb{E}|\mathbf{w}^H \tilde{\mathbf{h}}|^2 = 1$, we have further

$$R \geq \log_2(1 + \frac{p_u \beta \bar{\vartheta} MN}{1 + p_u \beta \bar{\vartheta}}) = \log_2(1 + \bar{\gamma}). \quad (22)$$

On the other hand, it follows easily that

$$\begin{aligned} R &= \mathbb{E} \log_2 \left(\frac{p_u \beta \bar{\vartheta} MN}{p_u \beta \bar{\vartheta} |\mathbf{w}^H \tilde{\mathbf{h}}|^2 + 1} \right) \\ &\leq \mathbb{E} \log_2(1 + p_u \beta \bar{\vartheta} MN) \\ &= \log_2(1 + \bar{\gamma}^L). \end{aligned} \quad (23)$$

If $E_u = MN p_u$ is fixed when $MN \rightarrow \infty$, by using the upper and lower bounds we easily obtain the desired result (20). ■

Theorem 1 reveals such a power scaling law that without degradation in the rate performance, the transmit power can be cut down by a factor of $\frac{1}{MN}$ when MN grows large.

C. Receive BF Scheme based on FF and MMSE Channel Estimation

In fact, we have just presented such a simple transmit/receive BF scheme that the transmitter and receiver only need to know partial information about the LOS component \mathbf{t} and \mathbf{r} , respectively. From another point of view, (9) also reveals that the considered MIMO system through the transmit BF is equivalent to a SIMO system. For this reason, using (9) as a starting point, we can also develop a receive BF (or say maximum-ratio combining (MRC)) scheme based on fast fading (FF) and minimum mean-squared error (MMSE) channel estimation by following the research ideas in [13] and [21]. The presupposition is that the receiver can have imperfect information about the scattered component (or say FF).

For the mentioned-above FF-based receive BF scheme, the equivalent channel vector \mathbf{g} needs to be estimated at receiver by using pilots from the transmitter. Its specular component $\bar{\mathbf{g}}$ (including β , ϑ , and $\bar{\mathbf{h}}$) is assumed to be constant over many coherence time intervals and known a priori. Therefore, only its scattered component $\tilde{\mathbf{g}}$ needs to be estimated.

Now let T denote the length of the coherence interval and $\tau < T$ denote the number of symbols used for the pilots. The used pilot sequence can be represented by a $\tau \times 1$ vector $\sqrt{p_p} \Phi$ satisfying $\Phi^H \Phi = 1$, with $p_p = \tau p_u$. Then the $M \times \tau$ received pilot matrix at the receiver is given by

$$\mathbf{Y}_p = \sqrt{p_p} \mathbf{g} \Phi^T + \mathbf{Z}_p \quad (24)$$

where $\mathbf{Z}_p = (z_{ij}^p)$ is an $M \times \tau$ matrix whose elements $\{z_{ij}^p\}$ are i.i.d., and $z_{ij}^p \sim \text{CN}(0, 1)$. If let $\tilde{\mathbf{Y}}_p = \mathbf{Y}_p - \sqrt{p_p} \bar{\mathbf{g}} \Phi^T$, then MMSE estimate of $\tilde{\mathbf{g}}$ is given by [13], [34]

$$\hat{\tilde{\mathbf{g}}} = \frac{\sqrt{p_p} \beta \tilde{\vartheta}}{1 + p_p \beta \tilde{\vartheta}} \tilde{\mathbf{Y}}_p \Phi^*. \quad (25)$$

Note that $(\cdot)^*$ denotes complex conjugate. We denote by $\Xi = \hat{\tilde{\mathbf{g}}} - \tilde{\mathbf{g}}$. By a derivation similar to that in [13], it can conclude that the random vector $\Xi = (\xi_i)$ is independent of $\hat{\mathbf{g}}$, and $\xi_i \sim \text{CN}(0, \delta_\xi^2)$, where $\delta_\xi^2 = \frac{\beta \tilde{\vartheta}}{1 + p_p \beta \tilde{\vartheta}}$. Moreover, let $\hat{\mathbf{g}} = (\hat{g}_i)$, and it follows easily that $\hat{g}_i \sim \text{CN}(0, \delta_g^2)$, where $\delta_g^2 = \frac{\beta^2 \tilde{\vartheta}^2 p_p}{1 + p_p \beta \tilde{\vartheta}}$.

After MMSE channel estimation, the weighting vector can be chose as $\mathbf{w} = \hat{\mathbf{g}}$. Then the combined signal at the receiver is given by

$$\begin{aligned} \hat{v} &= \hat{\mathbf{g}}^H (\sqrt{p_u} \mathbf{g} s + \mathbf{z}) \\ &= \sqrt{p_u} \hat{\mathbf{g}}^H \hat{\mathbf{g}} s - \sqrt{p_u} \hat{\mathbf{g}}^H \Xi s + \hat{\mathbf{g}}^H \mathbf{z}. \end{aligned} \quad (26)$$

At this time, the received SINR becomes

$$\hat{\gamma} = \frac{p_u \|\hat{\mathbf{g}}\|^2}{p_u \delta_\xi^2 + 1}. \quad (27)$$

Accordingly, the achievable rate for the BF scheme based on FF and MMSE channel estimation can be written as

$$\hat{R} = \frac{T - \tau}{T} \mathbb{E} \log_2 \left(1 + \frac{p_u \|\hat{\mathbf{g}}\|^2}{p_u \delta_\xi^2 + 1} \right). \quad (28)$$

Theorem 2: If ϑ and β are fixed, and $E_u = MN p_u$ is also fixed when $MN \rightarrow \infty$, then

$$\lim_{MN \rightarrow \infty} \hat{R} = \frac{T - \tau}{T} \lim_{MN \rightarrow \infty} R = \frac{T - \tau}{T} \lim_{MN \rightarrow \infty} \bar{R} = \frac{T - \tau}{T} \bar{R}^L. \quad (29)$$

Proof: With the help of the well-known law of large number, this result can be derived directly by using the following expressions

$$\delta_\xi^2 = \frac{\beta \tilde{\vartheta}}{1 + p_p \beta \tilde{\vartheta}}, \quad (30)$$

$$\mathbb{E} \|\bar{\mathbf{g}}\|^2 = MN \beta \tilde{\vartheta}, \quad (31)$$

$$\mathbb{E} \|\hat{\mathbf{g}}\|^2 = \frac{M \beta^2 \tilde{\vartheta}^2 p_p}{1 + p_p \beta \tilde{\vartheta}}, \quad (32)$$

and

$$\mathbb{E} \|\hat{\mathbf{g}}\|^2 = \mathbb{E} \|\bar{\mathbf{g}}\|^2 + \mathbb{E} \|\Xi\|^2 = MN \beta \tilde{\vartheta} + \frac{M \beta^2 \tilde{\vartheta}^2 p_p}{1 + p_p \beta \tilde{\vartheta}}. \quad (33)$$

Note that $p_p \rightarrow 0$ when $MN \rightarrow \infty$. ■

This theorem implies that the ergodic achievable rate of the LOS-based scheme can be higher than that of the FF-based scheme when M or N is very large.

III. UPLINK SINGLE-CELL MASSIVE-MIMO SYSTEMS

In Section II, we have considered a single-user massive-MIMO system. This simplifies the rate analysis, and it gives us important insights into how power can be scaled with the numbers of transmit and receive antennas. A natural problem is to what extent this power-scaling law still holds for multi-user Massive-MIMO systems. In this section, we will consider the problem and focus on the uplink single-cell scenario.

A. Uplink System Model

Let us consider an uplink single-cell MIMO system where the BS is equipped with M antennas and serves K users with each connected to N antennas. Then $M \times 1$ received signal vector at the BS is represented as

$$\mathbf{y} = \sqrt{p_u} \mathbb{G} \mathbb{X} + \mathbf{z} \quad (34)$$

where p_u is the average transmitted power of each user; \mathbb{G} is the $M \times NK$ channel matrix between the BS and the K users; \mathbb{X} is the symbol vector simultaneously transmitted by the K users; and \mathbf{z} still denotes a zero-mean AWGN vector with $\mathbb{E}[\mathbf{z}\mathbf{z}^H] = \mathbf{I}_M$.

The channel matrix \mathbb{G} consists of K sub-matrices as follows:

$$\mathbb{G} = [\mathbf{G}_1, \mathbf{G}_2, \dots, \mathbf{G}_K] \quad (35)$$

where the k -th sub-matrix \mathbf{G}_k is described as in Section II. A, i.e.,

$$\mathbf{G}_k = \sqrt{\beta_k} \mathbf{H}_k \quad (36)$$

where

$$\mathbf{H}_k = \sqrt{\bar{\vartheta}_k} \bar{\mathbf{H}}_k + \sqrt{\tilde{\vartheta}_k} \tilde{\mathbf{H}}_k \quad (37)$$

with $\bar{\vartheta}_k = \frac{\vartheta_k}{1+\vartheta_k}$, $\tilde{\vartheta}_k = \frac{1}{1+\vartheta_k}$, and $\vartheta_k \geq 0$ being the Rician K -factor of the k -th user. The entries of $\tilde{\mathbf{H}}_k$ are still modelled as i.i.d. $\text{CN}(0, 1)$ random variables. And $\bar{\mathbf{H}}_k$ is expressed as

$$\bar{\mathbf{H}}_k = \mathbf{r}_k \mathbf{t}_k^T. \quad (38)$$

In (III-A), \mathbf{r}_k and \mathbf{t}_k are written as

$$\mathbf{r}_k = [1, e^{j2\pi d \sin(\theta_k)}, \dots, e^{j2\pi(M-1)d \sin(\theta_k)}]^T \quad (39)$$

and

$$\mathbf{t}_k = [1, e^{j2\pi d_k \sin(\phi_k)}, \dots, e^{j2\pi(N-1)d_k \sin(\phi_k)}]^T \quad (40)$$

where d and d_k are the antenna spacings in wavelengths at the linear antenna arrays of the BS and the k user terminals, respectively, while θ_k and ϕ_k are the angles of arrival and departure of the channel specular component for the k -th user, respectively. We assume that $\theta_i \neq \theta_k$ when $i \neq k$.

B. Transmit/Receive BF Scheme based on Specular Component

The transmit/receive BF scheme based on specular component presented in Section II can be naturally extended to the uplink scenario.

For the k -th user, as in the single-user case, its transmit beamformer can be chosen as

$$\mathbf{b}_k = \frac{\mathbf{t}_k}{\sqrt{N}}, \quad k = 1, 2, \dots, K. \quad (41)$$

So the transmitted vector \mathbb{X} can be written as

$$\begin{aligned} \mathbb{X} &= [\mathbf{x}_1, \mathbf{x}_2, \dots, \mathbf{x}_K]^T \\ &= [\mathbf{b}_1 s_1, \mathbf{b}_2 s_2, \dots, \mathbf{b}_K s_K]^T \end{aligned} \quad (42)$$

where s_k is the symbol transmitted by the k -th user such that $\mathbb{E} s_k^H s_k = 1$. At the BS the received vector can be rewritten as

$$\mathbf{y} = \sqrt{p_u} \mathbf{G} \mathbf{s} + \mathbf{z} \quad (43)$$

where $\mathbf{s} = [s_1, s_2, \dots, s_K]$, and

$$\mathbf{G} = [\mathbf{g}_1, \mathbf{g}_2, \dots, \mathbf{g}_K] \quad (44)$$

with $\mathbf{g}_k = \mathbf{G}_k \mathbf{b}_k$.

(43) indicates that the uplink system through the processing of transmit BF can be reduced to a traditional uplink system with K single-antenna users, as discussed in [13] and [21]. Due to this reason, using (43) as a starting point, we can have three well-known linear detectors MRC, ZF and MMSE available, even under the constraint that the BS only knows the specular

component of channel matrix $\bar{\mathbf{G}}$. Now let $\mathbf{\Lambda}$ denote an $M \times K$ linear detecting matrix which only depends on $\bar{\mathbf{G}}$. Then these three linear detectors MRC, ZF and MMSE can be expressed as [13],

$$\mathbf{\Lambda} = \begin{cases} \bar{\mathbf{G}} & \text{for MRC;} \\ \bar{\mathbf{G}}(\bar{\mathbf{G}}^H \bar{\mathbf{G}})^{-1} & \text{for ZF;} \\ \bar{\mathbf{G}}(\bar{\mathbf{G}}^H \bar{\mathbf{G}} + (\sum_{k=1}^K \beta_k \tilde{\vartheta}_k + p_u^{-1}) \mathbf{I}_K)^{-1} & \text{for MMSE.} \end{cases} \quad (45)$$

As a matter of fact, these three detectors are equivalent to each other when $K = 1$.

After using the linear detector $\mathbf{\Lambda}$, the received vector \mathbf{y} becomes

$$\mathbf{v} = \mathbf{\Lambda}^H (\sqrt{p_u} \mathbf{G} \mathbf{s} + \mathbf{z}). \quad (46)$$

Let λ_k is the k -th element of $\mathbf{\Lambda}$. Then, the k -th element of \mathbf{v} is written in detail as

$$v_k = \sqrt{p_u} \lambda_k^H \bar{\mathbf{g}}_k s_k + \sqrt{p_u} \lambda_k^H \tilde{\mathbf{g}}_k s_k + \sqrt{p_u} \sum_{i=1, i \neq k}^K \lambda_k^H (\bar{\mathbf{g}}_i + \tilde{\mathbf{g}}_i) s_i + \lambda_k^H \mathbf{z}. \quad (47)$$

Thus the output statistical SINR is given by

$$\bar{\gamma}_k(K) = \frac{p_u |\lambda_k^H \bar{\mathbf{g}}_k|^2}{p_u \mathbb{E} |\lambda_k^H \tilde{\mathbf{g}}_k|^2 + p_u \sum_{i=1, i \neq k}^K \mathbb{E} |\lambda_k^H (\bar{\mathbf{g}}_i + \tilde{\mathbf{g}}_i)|^2 + \mathbb{E} |\lambda_k^H \mathbf{z}|^2}. \quad (48)$$

Proposition 2: For the MRC detector, we have

$$\bar{\gamma}_k(K) = \frac{p_u M N \beta_k \bar{\vartheta}_k}{1 + \frac{p_u N}{M} \sum_{i=1, i \neq k}^K \beta_i \bar{\vartheta}_i |\varrho_{ki}|^2 + p_u \sum_{i=1}^K \tilde{\vartheta}_i \beta_i} \quad (49)$$

where

$$\varrho_{ki} = \frac{1 - e^{jM\varphi_{ki}}}{1 - e^{j\varphi_{ki}}}, \quad \varphi_{ki} = 2\pi d(\sin(\theta_i) - \sin(\theta_k)). \quad (50)$$

Proof: For the MRC detector, $\lambda_k = \bar{\mathbf{g}}_k$. This result is easily derived by using the following expressions

$$|\lambda_k^H \bar{\mathbf{g}}_k|^2 = (M N \beta_k \bar{\vartheta}_k)^2, \quad (51)$$

$$\mathbb{E} |\lambda_k^H \mathbf{z}|^2 = M N \beta_k \bar{\vartheta}_k, \quad (52)$$

$$\mathbb{E} |\lambda_k^H \tilde{\mathbf{g}}_i|^2 = M N \beta_k \bar{\vartheta}_k \tilde{\vartheta}_i \beta_i, \quad (53)$$

and

$$\begin{aligned} |\lambda_k^H \bar{\mathbf{g}}_i|^2 &= |\sqrt{N \beta_k \bar{\vartheta}_k} \sqrt{N \beta_i \bar{\vartheta}_i} \mathbf{r}_k^H \mathbf{r}_i|^2 \\ &= N^2 \beta_k \bar{\vartheta}_k \beta_i \bar{\vartheta}_i \left| \frac{1 - e^{jM\varphi_{ki}}}{1 - e^{j\varphi_{ki}}} \right|^2 \\ &= N^2 \beta_k \bar{\vartheta}_k \beta_i \bar{\vartheta}_i |\varrho_{ki}|^2. \end{aligned} \quad (54)$$

■

Note that when MN grows large, $|\varrho_{ki}|^2 \leq \frac{4}{|1 - e^{j\varphi_{ki}}|^2}$ still keeps finite. Thus,

$$\lim_{M \rightarrow \infty} \frac{1}{M} |\varrho_{ki}|^2 = 0. \quad (55)$$

So in a LOS environment, we also have the following favorable propagation condition as if in a rich scattering environment [9], [13]

$$\lim_{M \rightarrow \infty} \frac{1}{M} \bar{\mathbf{G}}^H \bar{\mathbf{G}} = \mathbf{D} \quad (56)$$

where

$$\mathbf{D} = \text{diag}(\beta_1 \bar{\vartheta}_1, \beta_2 \bar{\vartheta}_2, \dots, \beta_K \bar{\vartheta}_K). \quad (57)$$

Furthermore, it follows from (56) and (45) that when M grows large the ZF and MMSE detectors can tend to that of the MRC. In reality, however, the implementation of the ZF and MMSE detectors involve a relatively complicated computation of finding the inverse of a large dimensional matrix, comparing with the MRC detector. Therefore, in what follows we focus on the simplest MRC detection scheme for the asymptotic statistical SINR analysis. We obtain the following results.

Corollary 4: Let $E_u = MNp_u$ be fixed when $M \rightarrow \infty$. Then

$$\lim_{M \rightarrow \infty} \bar{\gamma}_k(K) = \lim_{M \rightarrow \infty} \bar{\gamma}_k(1) = E_u \beta_k \bar{\vartheta}_k. \quad (58)$$

This corollary shows that the uplink system with multi-users has the same SINR limit as the one with single-user when the number of the BS antennas grows without bound. In other words, the very large antenna array deployed at the BS can eliminate intra-cell LOS interference and FF impact.

Corollary 5: When $N \rightarrow \infty$, let $E_u = MNp_u$ be fixed, M be finite, and $K > 1$ be fixed. Then

$$\lim_{N \rightarrow \infty} \bar{\gamma}_k(K) = \frac{E_u \beta_k \bar{\vartheta}_k}{1 + E_u M^{-2} c(K)} < \lim_{N \rightarrow \infty} \bar{\gamma}_k(1) = E_u \beta_k \bar{\vartheta}_k. \quad (59)$$

where $c(K) = \sum_{i=1, i \neq k}^K \beta_i \bar{\vartheta}_i |\varrho_{ki}|^2$.

This corollary implies that even though each user has a very large antenna array, the intra-cell LOS interference can not be mitigated while the FF impact can be eliminated.

Regarding (49), we define

$$\mathbb{E} \beta_i = \beta, \quad (60)$$

$$\mathbb{E}\bar{\vartheta}_i = \bar{\vartheta}, \quad (61)$$

$$\mathbb{E}\tilde{\vartheta}_i = \tilde{\vartheta}, \quad (62)$$

and

$$\mathbb{E}|\varrho_{ki}|^2 = |\varrho_k|^2. \quad (63)$$

When K is very large, the SINR in (49) can be approximated as

$$\bar{\gamma}_k(K) \approx \frac{p_u MN \beta_k \bar{\vartheta}_k}{1 + \frac{p_u N}{M} (K-1) \beta \bar{\vartheta} |\varrho_k|^2 + p_u K \tilde{\vartheta} \beta} \quad (64)$$

Corollary 6: Let $E_u = MNp_u$ be fixed. When $M \rightarrow \infty$ and $K \rightarrow \infty$, let $\frac{K}{M^\alpha} \rightarrow \iota$, and $\iota > 0$. If $0 < \alpha < 1$, then

$$\lim_{M \rightarrow \infty} \bar{\gamma}_k(K) = \lim_{M \rightarrow \infty} \bar{\gamma}_k(1) = E_u \beta_k \bar{\vartheta}_k. \quad (65)$$

And if $\alpha = 1$ and N be finite, then

$$\lim_{M \rightarrow \infty} \bar{\gamma}_k(K) = \frac{E_u \beta_k \bar{\vartheta}_k}{1 + E_u \iota \tilde{\vartheta} \beta / N} < \lim_{M \rightarrow \infty} \bar{\gamma}_k(1) = E_u \beta_k \bar{\vartheta}_k. \quad (66)$$

Corollary 6 indicates that the massive MIMO system by employing the transmit/receive BF scheme can also serve an infinite number of users. In particular, the very large antenna array at the BS can eliminate not only intra-cell LOS interference but also the FF impact as long as K and M^α ($0 < \alpha < 1$) grow with fixed ratio. If $\alpha = 1$, however, the system is still influenced by FF.

For the uplink system with $K > 1$ users, as in Section II, we can also present a receive BF scheme based on FF and MMSE channel estimation. When using the BF scheme, the ergodic achievable rate for the k -th user can be defined as

$$\hat{R}_k(K) = \frac{T - \tau}{T} \mathbb{E} \log_2(1 + \hat{\gamma}_k(K)) \quad (67)$$

where $\hat{\gamma}_k(K)$ denotes the receive SINR at the BS for the k -th user, T represents the coherence time of the channel in the terms of number of symbols and τ is the number of symbols used as pilots for the MMSE channel estimation [21]. On the other hand, if the system employs the LOS-based BF scheme, the corresponding achievable rate $R_k(K)$ has the following lower bound:

$$\begin{aligned} \bar{R}_k(K) &= \log_2 \left(1 + \frac{p_u \|\bar{\mathbf{g}}_k\|^4}{p_u \mathbb{E} |\bar{\mathbf{g}}_k^H \tilde{\mathbf{g}}_k|^2 + p_u \sum_{i=1, i \neq k}^K \mathbb{E} \|\bar{\mathbf{g}}_k (\bar{\mathbf{g}}_i + \tilde{\mathbf{g}}_i)\|^2 + \|\bar{\mathbf{g}}_k\|^2} \right) \\ &= \log_2(1 + \bar{\gamma}_k(K)). \end{aligned} \quad (68)$$

Moreover, if $E_u = MNp_u$ is fixed when $M \rightarrow \infty$, the upper bound of $R_k(K)$ can be represented as

$$\bar{R}_k^L = \lim_{M \rightarrow \infty} \bar{R}_k(K) = \log_2(1 + E_u \beta_k \bar{\vartheta}_k). \quad (69)$$

Theorem 3: Let $E_u = MNp_u$ be fixed when $M \rightarrow \infty$. Then

$$\lim_{M \rightarrow \infty} \hat{R}_k(K) = \frac{T - \tau}{T} \lim_{M \rightarrow \infty} \bar{R}_k(K) = \frac{T - \tau}{T} \bar{R}_k^L. \quad (70)$$

Proof: By Theorem 2 and Expressions (58), (68), and (69), it follows that

$$\lim_{M \rightarrow \infty} \hat{R}_k(K) \leq \lim_{M \rightarrow \infty} \hat{R}_k(1) = \lim_{M \rightarrow \infty} \frac{T - \tau}{T} \bar{R}_k(1) = \lim_{M \rightarrow \infty} \frac{T - \tau}{T} \bar{R}_k(K) = \frac{T - \tau}{T} \bar{R}_k^L. \quad (71)$$

Then we only need to prove $\lim_{M \rightarrow \infty} \hat{R}_k(K) \geq \lim_{M \rightarrow \infty} \frac{T - \tau}{T} \bar{R}_k(K)$.

Regarding the receive BF scheme based on FF and MMSE channel estimation, there exists such an extreme case where there is no pilot sequence to be used to estimate the scattered channel, i.e., $\tau = 0$. In this case, the BS will treat the LOS component as the channel estimate. This means that the LOS-based BF scheme can be viewed as a special case of the FF-based BF scheme. For this reason, we have,

$$\bar{R}_k(K) = \hat{R}_k(K)|_{\tau=0}. \quad (72)$$

Moreover, it can follow that

$$\hat{R}_k(K)|_{\tau=0} \leq \frac{T}{T - \tau} \hat{R}_k(K)|_{\tau>0}. \quad (73)$$

Thus

$$\frac{T - \tau}{T} \bar{R}_k(K) \leq \hat{R}_k(K). \quad (74)$$

So we can have the desired result

$$\lim_{M \rightarrow \infty} \hat{R}_k(K) = \lim_{M \rightarrow \infty} \frac{T - \tau}{T} \bar{R}_k(K). \quad (75)$$

Namely, Theorem 3 holds. ■

This theorem shows that for the uplink system with multi-users, the individual ergodic achievable rate with the LOS-based BF scheme can be higher than that with the FF-based scheme when the number of BS antennas is very large.

IV. DOWNLINK SCENARIO AND OTHER EXTENSION CONSIDERATION

A. Downlink Single-Cell Massive-MIMO

We next turn our attention to the downlink scenario in which the BS has M antennas and each of the K users has N antennas. We use \mathbf{G}_k^T to denote the downlink channel matrix from the BS to the k -th user such that \mathbf{G}_k can be described in (36). Then the received signal vector for the k -th user can be written as

$$\mathbf{y}_k = \sqrt{p_b} \mathbf{G}_k^T \mathbb{X} + \mathbf{z}_k \quad (76)$$

where p_b is the average transmitted power of the BS, \mathbb{X} is the symbol vector transmitted by the BS, and \mathbf{z}_k denotes a zero-mean AWGN vector with $\mathbb{E}[\mathbf{z}_k \mathbf{z}_k^H] = \mathbf{I}_N$.

For the downlink scenario, we also employ the conjugate BF precoding rather than ZF or MMSE precoding since the corresponding signal processing can be done distributedly at each antenna separately. When making use of the conjugate beamforming precoder, the transmitted vector can be given by

$$\mathbb{X} = \sum_{k=1}^K \frac{\mathbf{r}_k s_k}{\sqrt{KM}} \quad (77)$$

where \mathbf{r}_k is defined in (39), but different from the uplink scenario θ_k now denotes the angle of departure of the channel specular component while ϕ_k in (40) accordingly becomes the angle of arrival. The k -th user obtains by using the combiner $\frac{\mathbf{t}_k^H}{\sqrt{N}}$

$$v_k = \frac{\mathbf{t}_k^H}{\sqrt{N}} (\sqrt{p_b} \mathbf{G}_k^T \mathbb{X} + \mathbf{z}_k) \quad (78)$$

where \mathbf{t}_k is defined in (40). Furthermore, after some algebraic manipulations, v_k is written in detail as

$$v_k = \sqrt{\frac{p_b \beta_k \bar{\vartheta}_k}{K}} \left(\frac{\mathbf{t}_k^H \bar{\mathbf{H}}_k^T \mathbf{r}_k}{\sqrt{NM}} \right) s_k + \sqrt{\frac{p_b \beta_k \bar{\vartheta}_k}{K}} \left(\frac{\mathbf{t}_k^H \tilde{\mathbf{H}}_k^T \mathbf{r}_k}{\sqrt{NM}} \right) s_k + \sqrt{\frac{p_b \beta_k}{K}} \sum_{i=1, i \neq k}^K \left(\frac{\mathbf{t}_k^H \mathbf{G}_k^T \mathbf{r}_i}{\sqrt{NM}} \right) s_i + \left(\frac{\mathbf{t}_k^H \mathbf{z}_k}{\sqrt{N}} \right). \quad (79)$$

Proposition 3: For the k -th user, its output statistical SINR is given by

$$\bar{\gamma}_k(K) = \frac{\frac{p_b MN}{K} \beta_k \bar{\vartheta}_k}{1 + \frac{p_b N}{KM} \beta_k \bar{\vartheta}_k \sum_{i=1, i \neq k}^K |\varrho_{ki}|^2 + p_b \bar{\vartheta}_k \beta_k} \quad (80)$$

Proof: From (79) it follows that

$$\bar{\gamma}_k(K) = \frac{\frac{p_b \beta_k \bar{\vartheta}_k}{K} \left| \frac{\mathbf{t}_k^H \bar{\mathbf{H}}_k^T \mathbf{r}_k}{\sqrt{NM}} \right|^2}{\frac{p_b \beta_k \bar{\vartheta}_k}{K} \sum_{i=1, i \neq k}^K \left| \frac{\mathbf{t}_k^H \bar{\mathbf{H}}_k^T \mathbf{r}_i}{\sqrt{NM}} \right|^2 + \frac{p_b \beta_k \bar{\vartheta}_k}{K} \sum_{i=1}^K \mathbb{E} \left| \frac{\mathbf{t}_k^H \tilde{\mathbf{H}}_k^T \mathbf{r}_i}{\sqrt{NM}} \right|^2 + \mathbb{E} \left| \frac{\mathbf{t}_k^H \mathbf{z}_k}{\sqrt{N}} \right|^2}. \quad (81)$$

Thus the desired result can be obtained under the help of the following expressions

$$\frac{1}{\sqrt{NM}} \mathbf{t}_k^H \bar{\mathbf{H}}_k^T \mathbf{r}_k = \sqrt{NM}, \quad (82)$$

$$\frac{1}{\sqrt{N}} \mathbf{t}_k^H \mathbf{z}_k \sim \text{CN}(0, 1), \quad (83)$$

$$\frac{1}{\sqrt{NM}} \mathbf{t}_k^H \tilde{\mathbf{H}}_k^T \mathbf{r}_i \sim \text{CN}(0, 1), \quad (84)$$

and

$$\frac{1}{\sqrt{NM}} \mathbf{t}_k^H \bar{\mathbf{H}}_k^T \mathbf{r}_i = \sqrt{\frac{N}{M}} \varrho_{ki} \quad (85)$$

where $\varrho_{ki} = \frac{1 - e^{jM\varphi_{ki}}}{1 - e^{j\varphi_{ki}}}$, $\varphi_{ki} = 2\pi d(\sin(\theta_i) - \sin(\theta_k))$, and $\theta_i \neq \theta_k$. ■

For the asymptotic SINR analysis, we have the following results.

Corollary 7: When $M \rightarrow \infty$, let $E_b = MNp_b/K$ be fixed and K be finite. Then

$$\lim_{M \rightarrow \infty} \bar{\gamma}_k(K) = \lim_{M \rightarrow \infty} \bar{\gamma}_k(1) = E_b \beta_k \bar{\vartheta}_k. \quad (86)$$

Corollary 8: When $N \rightarrow \infty$, let $E_b = MNp_b/K$ be fixed, M and K be finite, and $K > 1$.

Then

$$\lim_{N \rightarrow \infty} \bar{\gamma}_k(K) = \frac{E_b \beta_k \bar{\vartheta}_k}{1 + E_b M^{-2} c_k(K)} < \lim_{N \rightarrow \infty} \bar{\gamma}_k(1) = E_b \beta_k \bar{\vartheta}_k. \quad (87)$$

where $c_k(K) = \beta_k \bar{\vartheta}_k \sum_{i=1, i \neq k}^K |\varrho_{ki}|^2$.

Corollary 9: Let $E_b = MNp_b/K$ be fixed. When $M \rightarrow \infty$ and $K \rightarrow \infty$, let $\frac{K}{M^\alpha} \rightarrow \iota$, $\iota > 0$.

If $0 < \alpha < 1$, Then

$$\lim_{M \rightarrow \infty} \bar{\gamma}_k(K) = \lim_{M \rightarrow \infty} \bar{\gamma}_k(1) = E_b \beta_k \bar{\vartheta}_k. \quad (88)$$

And if N be finite and $\alpha = 1$, then

$$\lim_{M \rightarrow \infty} \bar{\gamma}_k(K) = \frac{E_b \beta_k \bar{\vartheta}_k}{1 + E_b \iota \bar{\vartheta}_k \beta_k / N} < \lim_{M \rightarrow \infty} \bar{\gamma}_k(1) = E_b \beta_k \bar{\vartheta}_k. \quad (89)$$

Single-cell and multi-cell massive-MIMO systems have been investigated in time-division duplexing (TDD) mode [9], [13], [16]. For the downlink scenario under TDD mode, the channel matrix can be estimation through uplink pilot training. Similar to the discuss given in the uplink scenario, it can conclude that for each user its ergodic achievable rate of the BF scheme based on FF and MMSE channel estimation is not larger than that of the BF scheme only based on the specular component when the number of the BS antennas is large enough, namely,

Theorem 4: Let $E_b = MNp_b/K$ be fixed when $M \rightarrow \infty$, and let $p_p = p_b/K$. Then

$$\lim_{M \rightarrow \infty} \hat{R}_k(K) = \frac{T - \tau}{T} \lim_{M \rightarrow \infty} \bar{R}_k(K) = \frac{T - \tau}{T} \bar{R}_k^L. \quad (90)$$

B. Effect of Spacial Antenna Correlation

The aforementioned study is only limited in the spatially uncorrelated Rician fading model, which implies a rich scattering assumption. However, the rich scattering assumption is not always realistic and spatial correlation comes often into play. It has been shown that spatial antenna correlation changes drastically with the scattering environment, the distance between the transmitter and the receiver, the antenna configurations and the Doppler spread [31]. This motivates us to consider a spatially correlated Rician fading model and further observe if spatial correlation makes a great impact on the system performance.

In the single-cell uplink or downlink scenario, the subchannel matrix \mathbf{H}_k for the k -th user is now assumed to be of separately correlated Rician fading type, and then (37) can be rewritten as

$$\mathbf{H}_k = \sqrt{\tilde{\vartheta}_k} \bar{\mathbf{H}}_k + \sqrt{\tilde{\vartheta}_k} \boldsymbol{\Sigma}^{1/2} \tilde{\mathbf{H}}_k \boldsymbol{\Sigma}_k^{1/2} \quad (91)$$

where $\boldsymbol{\Sigma}$ and $\boldsymbol{\Sigma}_k$ are the correlation matrices of the BS terminal and the k -th user terminal, respectively, satisfying $\text{Tr}(\boldsymbol{\Sigma}) = M$ and $\text{Tr}(\boldsymbol{\Sigma}_k) = N$.

The scattered component makes an impact on the system performance through statistical properties of those random variables formed by weighting the scattered component, which have been given in (84) under the case without spacial correlation. When there exists spacial correlation, (84) need to be rewritten as

$$\frac{1}{\sqrt{NM}} \mathbf{t}_k^H (\boldsymbol{\Sigma}^{1/2} \tilde{\mathbf{H}}_k \boldsymbol{\Sigma}_k^{1/2})^T \mathbf{r}_i \sim \text{CN}(0, \delta_{ki}^2). \quad (92)$$

where

$$\delta_{ki}^2 = \frac{1}{MN} \|\mathbf{r}_i^H \boldsymbol{\Sigma}^{1/2}\|^2 \cdot \|\mathbf{t}_k^H \boldsymbol{\Sigma}_k^{1/2}\|^2. \quad (93)$$

In Section V, by numerical results we will make a comparison between the two cases with and without spacial correlation and examine the effect of spacial correlation on the individual rate.

C. Generalized Single-Link Model

So far we have investigated the transmission scheme based on transmit and receive conjugate BFs for single-cell massive MIMO systems through rank-1 Rician flat-fading channels. we can generalize the system model to the scenario including many factors such as distributed MIMO (

[14], [20], [23]), multi-cell ([15], [18]), heterogeneous network ([35]), spacial correlation ([5], [31], [36], [37]), high-rank Rician ([26], [38]), and frequency-Selective fading ([30], [39]). In the general scenario, a unified single-link transceiver model can be naturally formed by taking account of these factors, and noting such two facts that

a) A frequency selective MIMO channel can be converted into a set of parallel independent flat MIMO channels [30], [39];

b) For two independent complex random matrices following noncentral Gaussian distributions, their sum also follows a noncentral Gaussian distribution.

We consider a massive-MIMO link with N transmit antennas and M receive antennas, where NM is assumed to be very large. The $M \times 1$ received signal vector is represented as

$$\mathbf{y} = \sqrt{E}\mathbf{G}\mathbf{x} + \sum_{i=1}^L \sqrt{E_i}\mathbf{G}_i\mathbf{x}_i + \mathbf{z} \quad (94)$$

where \mathbf{z} still denotes the AWGN; $\mathbf{G} = \bar{\mathbf{G}} + \tilde{\mathbf{G}}$ denotes the $M \times N$ desired channel matrix following Rician fading distribution; \mathbf{G}_i denotes the i -th $M \times N_i$ interfering channel matrix with Rician fading distribution; E and E_i are the average transmitted powers of the desired user and the i -th interference user, respectively; and \mathbf{x} and \mathbf{x}_i are the transmitted symbol vector for the desired user and the i -th interference user, respectively.

Suppose that the transmitter and receiver only know the LOS component $\bar{\mathbf{G}}$. Then the optimal transmit/receive conjugate BF vectors \mathbf{b} and \mathbf{w} can be given by [32], [33]

$$\mathbf{w} = \bar{\mathbf{G}}\mathbf{b}, \quad \mathbf{b} = \mathbf{u}_{\max} \quad (95)$$

where \mathbf{u}_{\max} denotes eigenvector corresponding to the largest eigenvalue $\lambda(MN)$ of the quadratic form $\bar{\mathbf{G}}^H\bar{\mathbf{G}}$. We assume that $\mathbf{x}_i = \mathbf{b}_i s_i$ with $|\mathbf{b}_i^H \mathbf{b}_i| = 1$ and $\mathbb{E}\|s_i\|^2 = 1$.

This conjugate BF transmission scheme in the interference network would be attractive in practice if the following favorable propagation condition could be met:

$$\frac{\mathbb{E}|\mathbf{w}^H \sqrt{E}\tilde{\mathbf{G}}\mathbf{b}|^2}{\lambda(MN)} \leq \varepsilon_1, \quad (96)$$

$$\frac{\sum_{i=1}^L \mathbb{E}|\mathbf{w}^H \sqrt{E_i}\mathbf{G}_i\mathbf{b}_i|^2}{\lambda(MN)} \leq \varepsilon_2, \quad (97)$$

and

$$\frac{\mathbb{E}|\mathbf{w}^H \mathbf{z}|^2}{\lambda(MN)} \leq \varepsilon_3 \quad (98)$$

where ε_1 , ε_2 , and ε_3 are parameters involving quality of service (QoS) given in advance. By (96), (97) and (98), the output statistical SINR at the receiver is bounded by

$$\bar{\gamma} \geq \frac{E}{\varepsilon_1 + \varepsilon_2 + \varepsilon_3}. \quad (99)$$

The asymptotic analysis can be carried on by following a similar line of reasoning as in the single-cell case.

V. SIMULATION RESULTS

In this section, we present analytical results and simulation results for a single-cell with a radius of $r_m = 1000$ meters and K users distributed randomly and uniformly over the cell. It is assumed that there no user is closer to the BS than $r_h = 100$ meters. We first study the simple single-user case and then the uplink and downlink cases with multi-users. In all simulation, the large-scale fading coefficient β_k for the k -th user (or β) is always modelled as [13], [21],

$$\beta_k = z_k / (r_k / r_h)^v \quad (100)$$

where z_k is a log-normal random variable with standard deviation $\sigma = 8\text{dB}$, v denotes the path loss exponent and is set to be 3.8, and $r_k \in [r_h, r_m]$ denotes the distance between the underlying user and the BS. Note that $\mathbb{E}\beta_k = \bar{\beta}_k = 0.20479$. For simplicity, we always assume that all users have the identical Rician factor. Unless otherwise stated, the antenna spacings are assumed to be $d = d_r = 0.3$ and $d_k = d_t = 0.3$.

The lower bound of individual ergodic achievable rate $\bar{R}_k(K)$ is quite tight, especially at large M . Therefore, in the following, we will use $\bar{R}_k(K)$ to replace the exact rate $R_k(K)$ for all numerical work.

A. Single-user Massive-MIMO systems

We first validate Theorem 2 by Figure 1 and 2. If the transmitted data are modulated with orthogonal frequency division multiplexing (OFDM), as in [13] and [21], the coherence time of the channel can be chose to be $T = 196$ according to the LTE standard, and the length of uplink pilots can be chosen as $\tau = K$ for MMSE channel estimation. So $\frac{T-\tau}{T} = 195/196$. In order to make a convenient comparison, however, below we consider to compare \bar{R} with $\hat{R}^\tau = \frac{T}{T-\tau}\hat{R}$ rather than \hat{R} when the large-scale fading coefficient and the angle of arrival are set to be $\beta = \bar{\beta} = 0.20479$ and $\theta = \pi/4$, respectively.

Assuming that $N=10$, $E_u = 20\text{dB}$ and $\vartheta = 5\text{dB}$, Figure 1 plots \bar{R} and \hat{R}^τ as two functions of the number of receive antennas M . For further comparison, Figure 1 also plots the rate limit \bar{R}^\perp and a random example of the instantaneous rate when the FF-based scheme is used. As expected, Figure 1 shows such a power scaling law that as M grows large, both of the rates \bar{R} and \hat{R}^τ tend to the rate limit \bar{R}^\perp . It can be seen from this figure that the two rates are close to each other when M is relatively large while \hat{R}^τ is higher than \bar{R} when M is relatively small. Moreover, the random rate curve has a large fluctuation, but still tends to the limit result when M is very large.

Furthermore, in the case where both β and θ are assume to be random, Figure 2 plots $\mathbb{E}\bar{R}$ and $\mathbb{E}\hat{R}^\tau$ as the number of receive antennas M changes. The behavior of the two rates with LOS- and FF-based schemes is similar to that in the case where β and θ are fixed. From Figure 1 and Figure 2, however, it can be found that the following approximation result does not hold

$$\mathbb{E}\bar{R} \approx \log_2(1 + \mathbb{E}(E_u\beta\bar{\vartheta})) = \log_2(1 + (E_u\bar{\beta}\bar{\vartheta})). \quad (101)$$

When β is random, we next consider to verify Proposition 1 and its corollaries by Figure 3, Figure 4 and Figure 5. Under the case of $N = 10$ and $\vartheta = 5\text{dB}$, Figure 3 shows that although $\mathbb{E}\bar{R}$ improves with an increasing p_u , the amount of improvement becomes smaller and smaller. In Figure 4, we set $N = 10$ and $E_u = 20\text{dB}$. It can be observed from Figure 4 that the average rate $\mathbb{E}\bar{R}$ increases as ϑ increases, but the amount of rate improvement becomes smaller and smaller. In Figure 5, we assume that $\vartheta = 5\text{dB}$ and $E_u = 20\text{dB}$. Although the two rates with $N = 10$ and $N = 1$ can increase as M grows from 10 to 100, only the one with $N = 10$ is close to the theoretical limit when $M = 100$. Moreover, it is interestingly found in Figure 5 that the rate result with $N = 10$ and $M = 10$ is equal to the rate result with $N = 1$ and $M = 100$. This phenomena can be explained by Corollary 3, and gives us a suggestion for practical MIMO configuration.

B. Uplink Massive-MIMO systems

We now turn our attention to the uplink scenario, and first make a comparison among the MMSE, ZF, and MRC linear detection schemes. When $N = 3$, $K = 10$, $\vartheta_k = 5\text{dB}$, $\beta_k = 0.20479$, and $k = 1, 2, \dots, K$, Figure 6 plots three curves about the average sum rate for $E_u = 30, 20, 10\text{dB}$. As expected, simulation results show that the MMSE scheme is always optimal

among them. When $M \geq 30$, however, the ZF scheme and the MMSE scheme can perform similarly in the terms of the sum rate, and outperform the MRC scheme for $E_u = 30\text{dB}$ and $E_u = 20\text{dB}$. When $E_u = 10\text{dB}$, all of these three scheme have similar performance. This means that the MRC tends to the optimal MMSE with a decreasing E_u .

We set $N = 3$, $E_u = 20\text{dB}$, $\vartheta_k = 5\text{dB}$, $\beta_k = 0.20479$, and $k = 1, 2, \dots, K$. In this case, we consider to corroborate Theorem 3 by comparing the sum rate of the LOS-based scheme with that of the FF-based scheme. For $K = 50, 10, 2$, Figure 7 plots the two sum rates of $\sum_{k=1}^K \bar{R}_k(K)$ and $\sum_{k=1}^K \hat{R}_k^\tau(K) = \frac{T}{T-\tau} \sum_{k=1}^K \hat{R}_k(K)$ as M increases from 30 to 300. For comparison, three curves are also plotted by using the corresponding limit results $K\bar{R}^L$. From Figure 7 it can be observed that the two LOS- and FF-based schemes perform similarly, and their sum rates tend to the corresponding limit results for the three different values of K . However, as K increases, the inter-user interference becomes stronger and stronger, and thus the speed of convergence becomes slower and slower even although M is very large.

It should be noticed that in Figures 6 and 7 the angle of arrival for the k -th user is set to be $\theta_k = \frac{\pi}{2} + \frac{2k-1}{2K}$, $k = 1, 2, \dots, K$.

we examine Corollary 5 by Figure 8, assuming that the angle of arrival for the k -th user θ_k is random. We further assume that $M = 20$, $K = 10$, $E_u = 20\text{dB}$, $\vartheta_k = 5\text{dB}$, $\beta_k = 0.20479$, and $k = 1, 2, \dots, K$. Different from the single-user case, the individual rate limit with $M \rightarrow \infty$ is obviously higher than the one with $N \rightarrow \infty$. Even when N is not very large, the exact individual rate can be quite close to the latter.

C. Impacts of the number of users, correlation coefficients, and antenna spacings

Finally, we conduct experiments for the downlink scenario and analyze the impact of the number of users, correlation coefficients, and antenna spacings on the rate performance. In Figures 9-11, we assume that the angle of arrival for the k -th user θ_k is random.

In order to verify Corollary 9 in Section IV, Figure 9 plots the average individual rate as a function of the number of BS for three different values of $\alpha = 1/2, 3/4, 1$ under the case with $\iota = 1/2$. In Figure 9, we assume that $N = 2$, $E_u = 10\text{dB}$, $\vartheta_k = 5\text{dB}$, $\beta_k = 0.20479$, and the rate limit is included for comparison. As expected, when α decreases, the number of users also decreases, and the average individual rate be closer to the rate limit. On the other hand, for a fixed $\alpha \in (0, 1)$ the average individual rate can improve as the number of BS antennas grows

large from 60 to 600, but the amount of improvement is extremely small. When α is fixed to be one, however, the average individual rate keeps almost unchange as the number of BS antennas grows large from 200 to 600.

In what follows, we observe by simulation the impact of spacial correlation and antenna array structure on the achievable rate in the downlink scenario.

In order to provide an assessment of the influence of spacial correlation, Figure 10 plots the average individual rate as a function of the number of BS antennas for various spacial correlation cases when $\beta_k = 0.20479$, $K = 10$, $E_b = 20\text{dB}$ and $N = 10$. In Figure 10, we employ exponential correlation model such that the BS correlation matrix and the user correlation matrix can be expressed as $(g_b^{|i-j|})$ and $(g_u^{|i-j|})$ where $g_b \in [0, 1]$ and $g_u \in [0, 1]$ denote their correlation coefficients. Note that $g_b = 0$ (or $g_u = 0$) indicate that there is no spacial correlation at the BS antenna array (or user antenna array). It can be clearly seen from Figure 10 that when $\vartheta_k = 5\text{dB}$, the four rate curves plotted for four different values of the BS correlation coefficient $g_b = 0, 0.3, 0.6, 0.9$ are quite similar under the case of $g_u = 0$. This means that the impact of the BS spacial correlation on the rate can be negligible. For $\vartheta_k = -10\text{dB}$, Figure 10 also plots four rate curves which correspond the four cases as follows: i) the uncorrelated case of $(g_b = 0, g_u = 0)$; ii) the semi-correlated case of $(g_b = 0, g_u = 0.5)$; iii) the semi-correlated case of $(g_b = 0.5, g_u = 0)$, and iv) the double-correlated case of $(g_b = 0.5, g_u = 0.5)$. The four rate curves are obviously similar. This implies that neither the BS spacial correlation nor the user spacial correlation make a serious impact on the rate performance.

To examine the influence of antenna spacings on the rate performance of uncorrelated MIMO systems, Figure 11 depicts the average individual rate against the number of BS antennas for various antenna spacing cases when $\beta_k = 0.20479$, $d_k = 0.3$, $K = 10$, $N = 3$, and $E_b = 20\text{dB}$. It can be clearly seen from Figure 11 that as d grows large from 0.05 to 24, the average individual rate increases, but the amount of increasing gradually becomes smaller. In particular, the rate values with $d = 2.4$ is quite close to the ones with $d = 24$. It is interesting to notice that the individual rate with $d = 0.05$ and $M = 300$ is an accurate approximation of that with $d = 2.4$ and $M = 30$. This example implies such a power scaling law that the transmit power needed in the former case is one tenth of the one needed in the latter case.

For comparison with the correlation case, Figure 11 also depicts the average individual rate against M for the following three correlation cases: i) $g_b = 0.5$ and $g_u = 0$ when $d = 0.05$ and

$d_k = 0.3$; ii) $g_b = 0.5$ and $g_u = 0.5$ when $d = 0.3$ and $d_k = 0.01$; iii) $g_b = 0.5$ and $g_u = 0$ when $d = 24$ and $d_k = 0.3$. Similar to the case with $d = 0.3$ and $d_k = 0.3$ shown in Figure 10, it concludes that spacial correlation has no serious influence on the rate performance.

VI. CONCLUSION

In this paper, we have investigated the LOS-based conjugate BF transmission scheme for massive-MIMO systems over Rician fading channels, derived some expressions of the statistical SINR, and presented several power scaling laws for several cases under the help of these expressions. By comparison with pure Rayleigh fading environments, it can be found that massive MIMO systems are more suitable to be deployed in Rician fading environments, especially when the LOS component is strong.

Numerical results have been conducted only by the system models with some ideal assumptions. In future work, we will examine our theoretical analysis based on more practical system models.

REFERENCES

- [1] A. Goldsmith, S. A. Jafar, N. Jindal, and S. Vishwanath, "Capacity Limits of MIMO Channels," *IEEE J. Sel. Areas Commun.*, Vol. 21, No. 5, pp. 684-702, June 2003.
- [2] D. Gesbert, M. Kountouris, R. W. Heath Jr., C.-B. Chae, and T. Sälzer, "Shifting the MIMO paradigm," *IEEE Sig. Proc. Mag.*, vol. 24, no. 5, pp. 36-46, 2007.
- [3] C. B. Peel, B. M. Hochwald and A. L. Swindlehurst, "A vector-perturbation technique for near-capacity multiantenna multiuser communication-part I: channel inversion and regularization," *IEEE Trans. Commun.*, vol. 53 no. 1, pp. 195-202, Jan.2005.
- [4] P. Wang and P. Li, "On Maximum eigenmode beamforming and multi-user gain," *IEEE Trans. Inf. Theory*, vol. 57, no. 7, pp.4170-4186, Jul. 2011.
- [5] C. K. Wen, S. Jin, and K. K. Wong, "On the Sum-Rate of Multiuser MIMO Uplink Channels with Jointly-Correlated Rician fading," *IEEE Trans. Commun.*, Vol. 59, No. 10, pp. 2883-2895, Oct. 2011.
- [6] N. Ravindran, N. Jindal, and H. C. Huang, "Beamforming with finite rate feedback for LOS MIMO downlink channels," in *Proc. IEEE Global Telecommun. Conf. (GLOBECOM)*, Nov. 2007, pp. 4200C4204.
- [7] T. Yoo and A. Goldsmith, "On the optimality of multiantenna broadcast scheduling using zero-forcing beamforming," *IEEE J. Sel. Areas Commun.*, vol. 24, no. 3, pp. 528-541, Mar.2006.
- [8] A. Wiesel, Y. C. Eldar and S. Shamai, "Zero-forcing precoding and generalized inverses," *IEEE Trans. Signal Process.*, vol. 56, no. 9, pp. 4409-4418, Sep. 2008.
- [9] T. L. Marzetta, "Noncooperative cellular wireless with unlimited numbers of base station antennas," *IEEE Trans. Wireless Commun.*, vol. 9, no. 11, pp. 3590-3600, Nov. 2010.

- [10] F. Rusek, D. Persson, B. K. Lau, E. G. Larsson, T. L. Marzetta, O. Edfors, and F. Tufvesson, "Scaling up MIMO: Opportunities and challenges with very large arrays," *IEEE Signal Process. Mag.*, vol. 30, no. 1, pp. 40-60, Jan. 2013.
- [11] L. Lu, G. Y. Li, A. L. Swindlehurst, A. Ashikhmin, and R. Zhang, "An overview of massive MIMO: benefits and challenges," *IEEE J. Sel. Topics Signal Process.*, vol. 62, no.5, pp. 742-758, Oct. 2014.
- [12] X. Gao, O. Edfors, F. Rusek, and F. Tufvesson, "Linear Pre-Coding Performance in Measured Very-Large MIMO Channels," in *Proc. IEEE Vehi. Tech. Conf. (VTC)*, San Francisco, CA, US, Sept. 2011, pp. 1-5.
- [13] H. Q. Ngo, E. G. Larsson, and T. L. Marzetta, "Energy and spectral efficiency of very large multiuser MIMO systems," *IEEE Trans. Commun.*, vol. 61, no. 4, pp. 1436-1449, Apr. 2013.
- [14] M. Matthaiou, C. Zhong, M. R. McKay, and T. Ratnarajah, "Sum rate analysis of ZF receivers in distributed MIMO systems," *IEEE J. Sel. Areas Commun.*, vol. 31, no. 2, pp. 180-191, Feb. 2013.
- [15] H. Q. Ngo, E. G. Larsson, and T. L. Marzetta, "The multicell multiuser uplink with very large antenna arrays and a finite-dimensional channel," *IEEE Trans. Commun.*, vol. 61, no. 6, pp. 2350-2361, June 2013.
- [16] J. Hoydis, S. Ten Brink, and M. Debbah, "Massive MIMO: How many antennas do we need?" *IEEE J. Sel. Areas Commun.*, vol. 31, no. 2, pp. 160-171, Feb. 2013.
- [17] H. Yin, D. Gesbert, M. Filippou, and Y. Liu, "A Coordinated Approach to Channel Estimation in Large-scale Multiple-antenna Systems," *IEEE J. Sel. Areas Commun.*, vol. 31, no. 2, pp. 264-273, Feb. 2013.
- [18] H. Q. Ngo, T. L. Marzetta, and E. G. Larsson, "Analysis of the pilot contamination effect in very large multicell multiuser MIMO systems for physical channel models," in *Proc. IEEE Int. Conf. Acoustics, Speech, Signal Process. (ICASSP)*, May 2011, pp. 3464-3467.
- [19] H. Q. Ngo and E. G. Larsson, "EVD-Based Channel Estimations for Multicell Multiuser MIMO with Very Large Antenna Arrays," *IEEE Int'l Conf. on Acoustics, Speed and Signal Processing (ICASSP)*, Kyoto, Japan, Mar. 2012.
- [20] J. Zhang, C. -K. Wen, S. Jin, X. Gao, and K. -K. Wong, "On capacity of large-scale MIMO multiple access channels with distributed sets of correlated antennas," *IEEE J. Sel. Areas Commun.*, vol. 31, no. 2, pp. 133-148, 2013.
- [21] Q. Zhang, Z. Lu, S. Jin, K. -K. Wong, H. Zhu, M. Mattaiou, "Power scaling of massive MIMO systems with arbitrary -rank channel means and imperfect CSI," in *proc. IEEE Global Telecommun. Conf. (GLOBECOM)*, Dec.2013, pp. 4262-4267.
- [22] Y. Liu, Z. Tan, and G. Y. Li, "Single-carrier modulation with ML equalization for large-scale antenna systems over Rician fading channels," in *Proc. IEEE Int. Conf. Acoustics, Speech, Signal Process. (ICASSP)*, May 2014.
- [23] J. Zhang, X. Yuan, and P. Li, "Hermitian precoding for distributed MIMO systems with individual channel state information," *IEEE J. Sel. Areas Commun.*, vol. 31, no. 2, pp. 241-250, Feb. 2013.
- [24] H. Yang and T. L. Marzetta, "Performance of conjugate and zero-forcing beamforming in large-scale antenna systems," *IEEE J. Sel. Areas Commun.*, vol. 31, no. 2, pp. 172-179, Feb. 2013.
- [25] Y.-G. Lim, C.-B. Chae, G. Caire, "Performance analysis of massive MIMO for cell-boundary users," [online]. Available: <http://arxiv.org/abs/1309.7817>.
- [26] M. Matthaiou, P. D. Kerret, G. K. Karagiannidis, and J. A. Nossek, "Mutual information statistics and beamforming performance analysis of optimized LoS MIMO systems," *IEEE Trans. Commun.*, vol. 58, no. 11, pp.180 – 191, Nov. 2010.
- [27] J. Hoydis, M. Kobayashi, and M. Debbah, "Green small-cell networks," *IEEE Vehi. Tech. Mag.*, vol. 6, no. 1, pp. 37-43, 2011.
- [28] T. Zahir, K. Arshad, A. Nakata, and K. Moessner, "Interference management in femtocells," *IEEE Commun. Surveys Tutorials*, vol. 15, no. 1, pp. 293-311, 1st quarter 2013.

- [29] F. R. Farrokhi, G. J. Foschini, A. Lozano, and R. A. Valenzuela, "Link optimal space-time processing with multiple transmit and receive antennas," *IEEE Commun. Lett.*, vol. 5, pp. 85-87, Mar. 2001.
- [30] S. Jin, X. Gao, and X. You, "On the ergodic capacity of rank-1 Ricean fading MIMO channels," *IEEE Trans. Inf. Theory*, vol. 53, no. 2, pp. 502-517, Feb. 2007.
- [31] G. Taricco and E. Riegler, "On the ergodic capacity of correlated Rician fading MIMO channels with interference," *IEEE Trans. Inf. Theory*, vol. 57, no. 7, pp. 4123-4137, July 2011.
- [32] D.-W. Yue and Q. T. Zhang, "Generic approach to the performance analysis of correlated transmit/receive diversity MIMO systems with/without co-channel interference," *IEEE Trans. Inf. Theory*, vol. 56, no. 3, pp. 1147-1157, Mar. 2010.
- [33] M. Kang and M.-S. Alouini, "Quadratic forms in complex Gaussian matrices and performance analysis of MIMO systems with cochannel interference," *IEEE Trans. Wireless Commun.*, vol. 3, no. 2, pp. 418-431, 2004.
- [34] H. Hassibi and B. M. Hochwald, "How much training is needed in multiple-antenna wireless links?" *IEEE Trans. Inf. Theory*, vol. 49, No. 4, pp. 951-963, Apr. 2003.
- [35] Y. Jeong, H. Shin, and M. Z. Win, "Superanalysis of optimum combining with application to femtocell networks," *IEEE J. Sel. Areas Commun.*, vol. 30, no. 3, pp. 509-524, 2012.
- [36] E. Riegler and G. Taricco, "Asymptotic Statistics of the Mutual Information for Spatially Correlated Rician Fading MIMO Channels with Interference," *IEEE Trans. Inf. Theory*, vol. 56, no. 4, pp. 1542-1559, Apr. 2010.
- [37] C. Siriteanu, S. D. Blostein, A. Takemura, H. Shin, S. Yousefi, and S. Kuriki, "Exact MIMO zero-forcing detection analysis for transmit-correlated Rician fading," *IEEE Trans. Wireless Commun.*, accepted, Dec. 2013. [online]. Available: <http://arxiv.org/abs/1307.2958>.
- [38] Bøhagen, P. Orten, and G. E. Øien, "Design of capacity-optimal high-rank line-of-sight MIMO channels," *IEEE Trans. Wireless Commun.*, vol. 6, no. 4, pp. 1420-1425, Apr. 2007.
- [39] M. R. McKay and I. B. Collings, "On the capacity of frequency -flat and frequency-selective Rician MIMO channels with single-ended correlation," *IEEE Trans. Wireless Commun.*, vol. 5, no. 8, pp. 2038-2043, Aug. 2006.

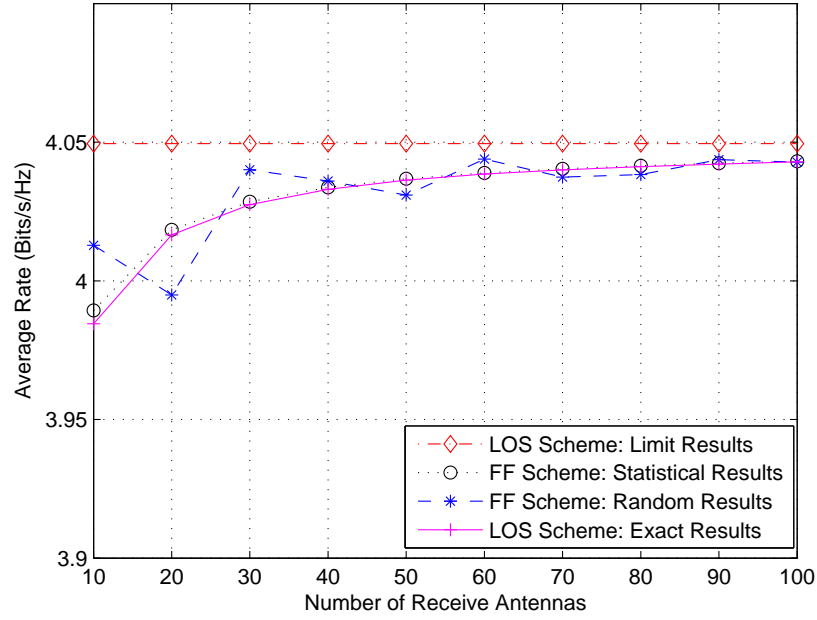


Fig. 1. Average rate versus the number of receiver antennas in the single user scenario for making a comparison between the LOS- and FF-based schemes when the large-scale fading parameter is fixed.

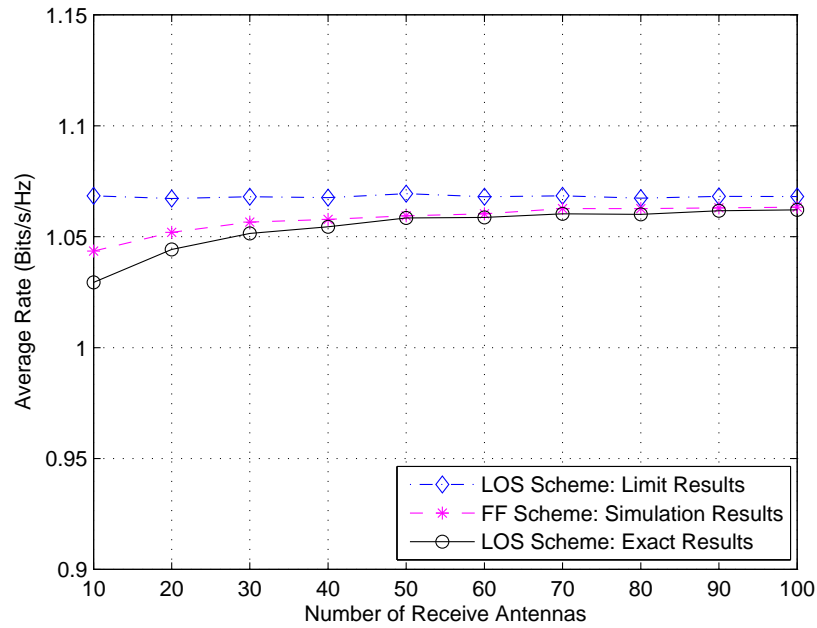


Fig. 2. Average rate versus the number of receiver antennas in the single user scenario for making a comparison between the LOS- and FF-based schemes when the large-scale fading parameter is random.

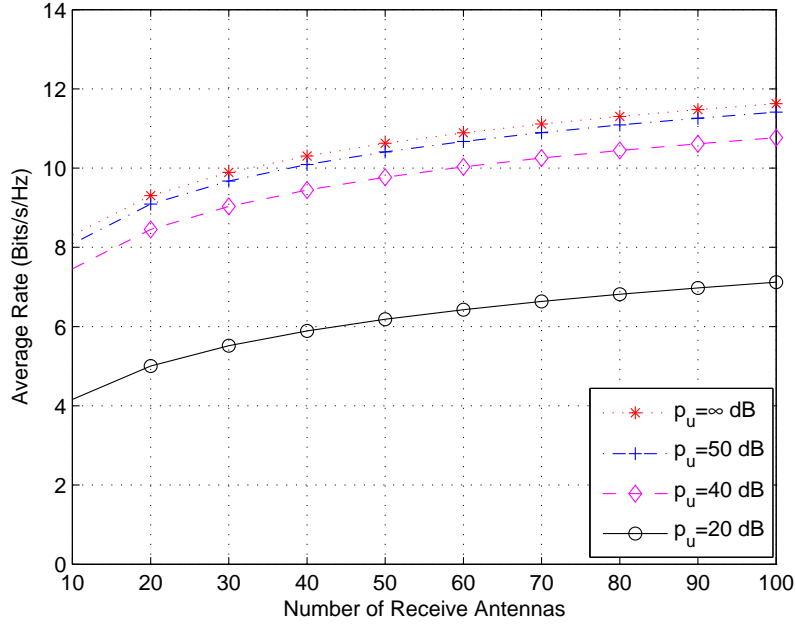


Fig. 3. Average rate versus the number of receiver antennas in the single user scenario for different transmit powers.

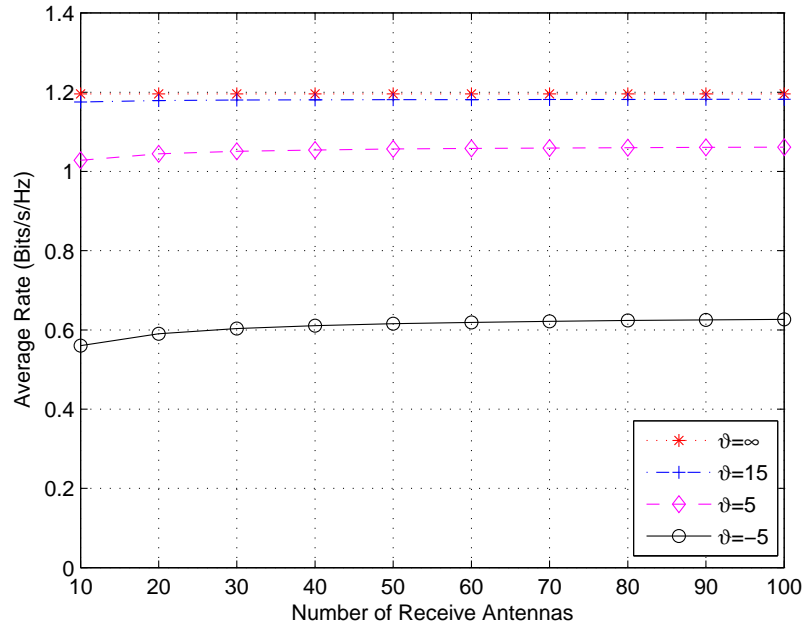


Fig. 4. Average rate versus the number of receiver antennas in the single user scenario for different Rician factors.

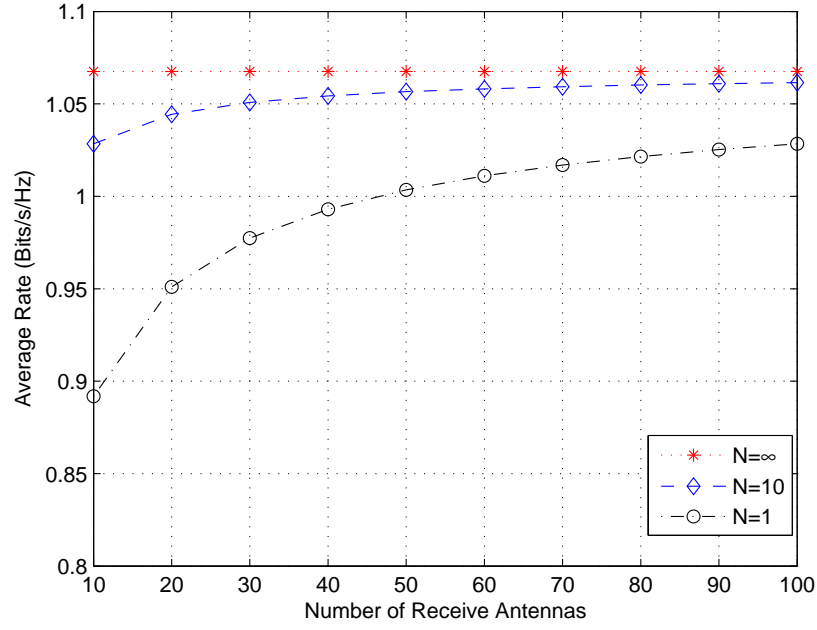


Fig. 5. Average rate versus the number of receiver antennas in the single user scenario for different numbers of transmit antennas.

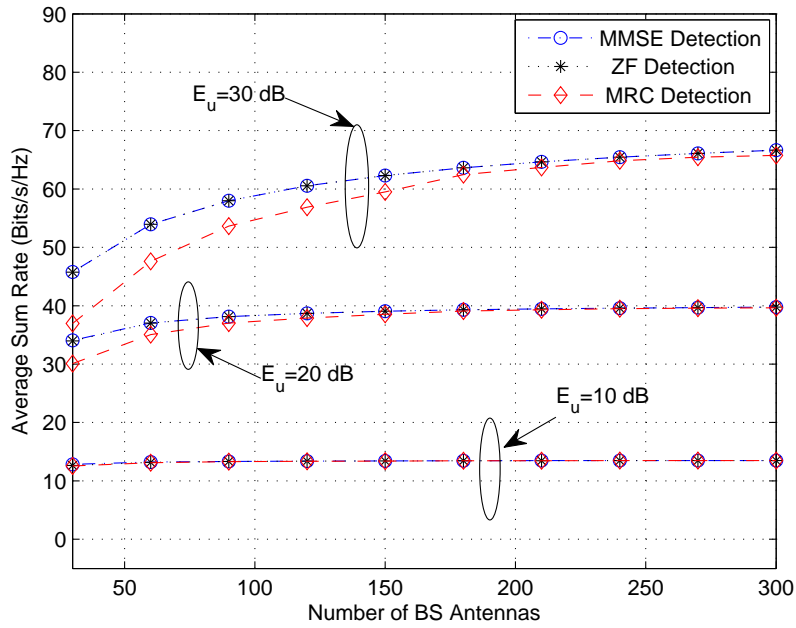


Fig. 6. Average sum rate versus the number of BS antennas in the uplink scenario for making a comparison among BF, ZF and MMSE linear detectors when several values of E_u are used.

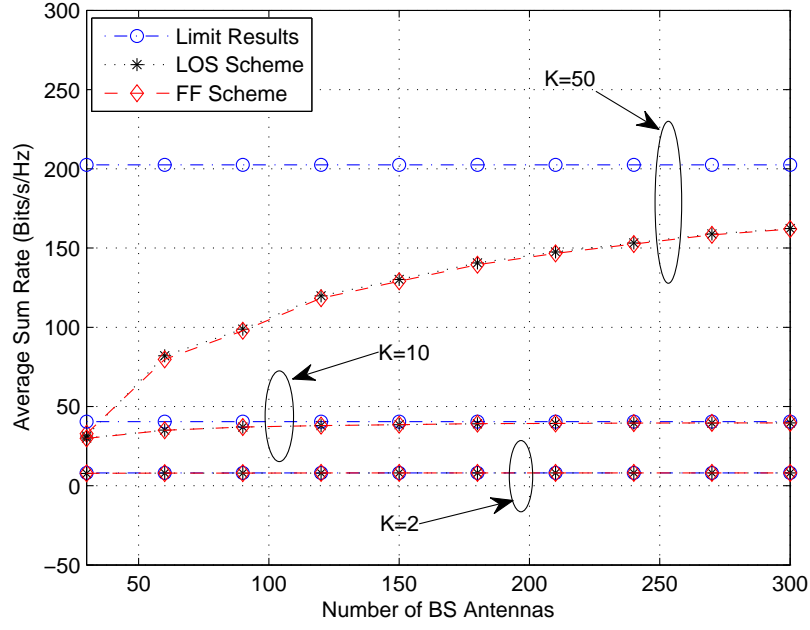


Fig. 7. Average sum rate versus the number of BS antennas in the uplink scenario for making a comparison between the LOS- and FF-based schemes when several values of K are used.

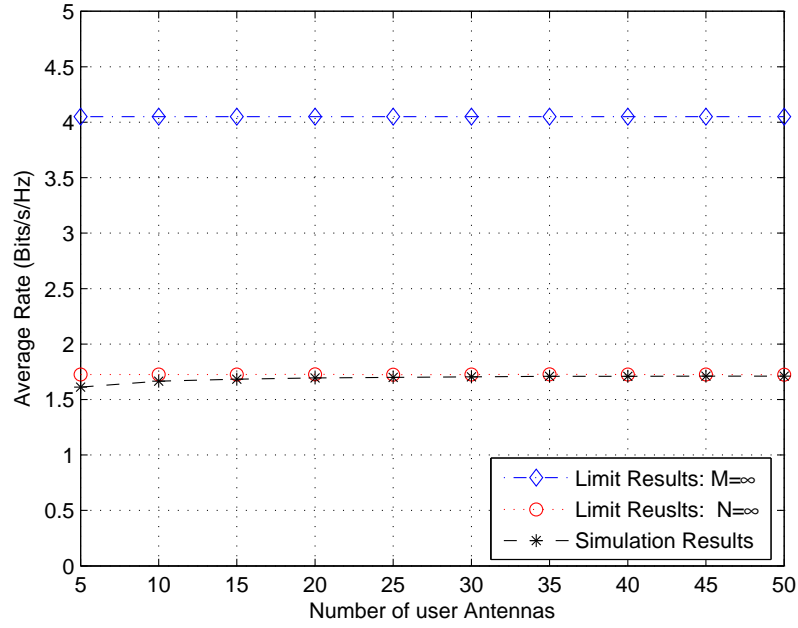


Fig. 8. Average individual rate versus the number of user antennas in the uplink scenario.

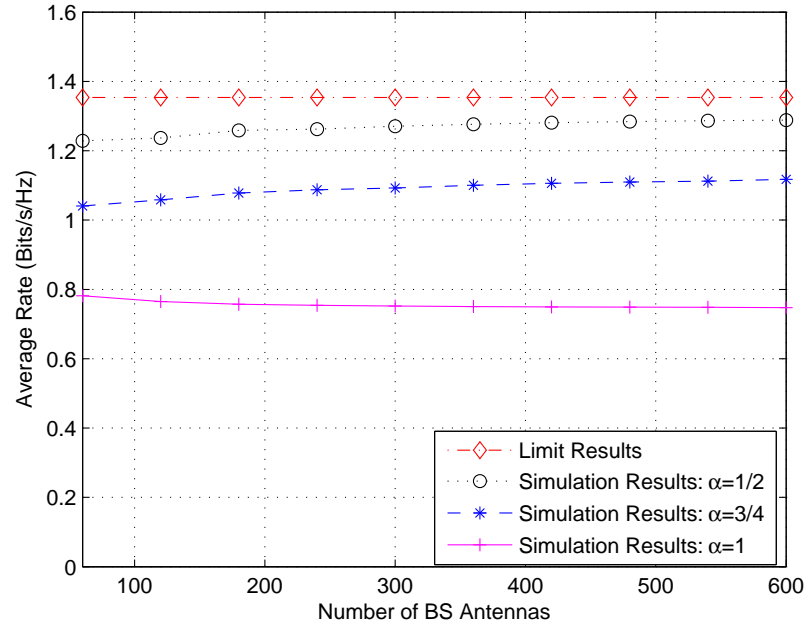


Fig. 9. Average individual rate versus the number of BS antennas in the downlink scenario for different values of the parameter α .

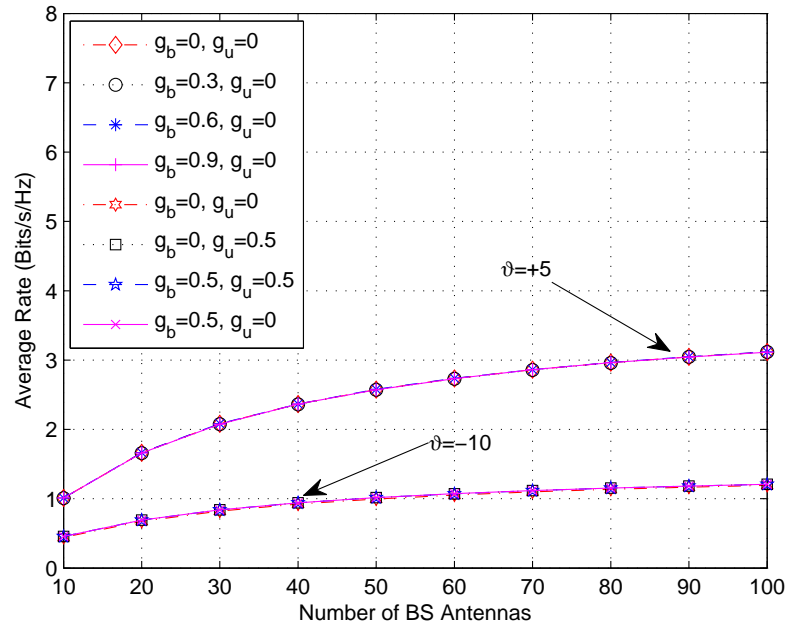


Fig. 10. Average individual rate versus the number of BS antennas in the downlink scenario for various pairs of spatial correlation coefficients.

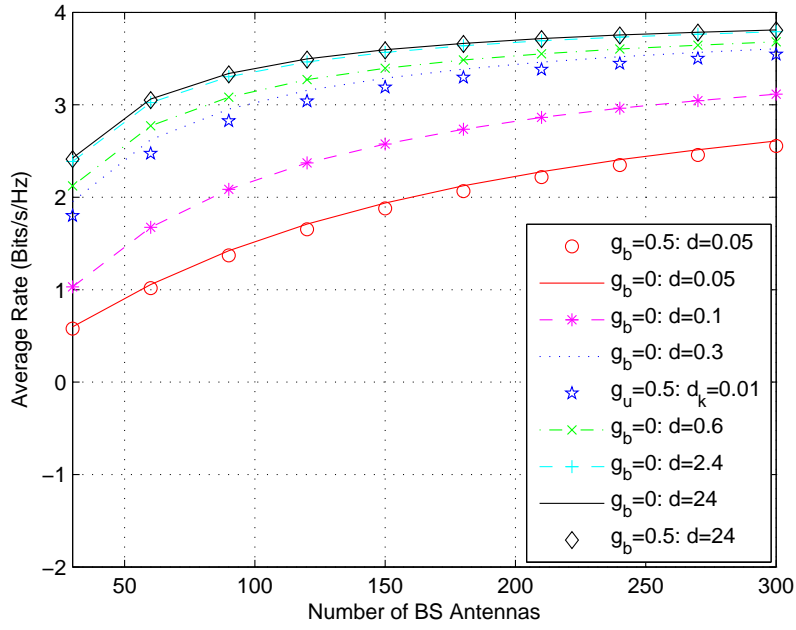


Fig. 11. Average individual rate versus the number of BS antennas in the downlink scenario for various values of antenna spacing.